PROCEEDINGS OF THE ROYAL SOCIETY B

Proc. R. Soc. B (2007) **274**, 323–331
doi:10.1098/rspb.2006.3738
Published online 31 October 2006

Foetal age determination and development in elephants

Thomas Hildebrandt[1,*], Barbara Drews[1], Ann P. Gaeth[2], Frank Goeritz[1], Robert Hermes[1], Dennis Schmitt[3], Charlie Gray[4], Peter Rich[4], Wolf Juergen Streich[1], Roger V. Short[2,5] and Marilyn B. Renfree[2]

[1]*Institute for Zoo and Wildlife Research, Alfred-Kowalke-Straße 17 10315 Berlin, Germany*
[2]*Department of Zoology, and* [5]*Faculty of Medicine, University of Melbourne, Melbourne, Victoria 3010, Australia*
[3]*Department of Agriculture, Missouri State University, Springfield, MO 65897, USA*
[4]*African Lion Safari, Cambridge, Ont, Canada N1R 5S2*

Elephants have the longest pregnancy of all mammals, with an average gestation of around 660 days, so their embryonic and foetal development have always been of special interest. Hitherto, it has only been possible to estimate foetal ages from theoretical calculations based on foetal mass. The recent development of sophisticated ultrasound procedures for elephants has now made it possible to monitor the growth and development of foetuses of known gestational age conceived in captivity from natural matings or artificial insemination. We have studied the early stages of pregnancy in 10 captive Asian and 9 African elephants by transrectal ultrasound. Measurements of foetal crown–rump lengths have provided the first accurate growth curves, which differ significantly from the previous theoretical estimates based on the cube root of foetal mass. We have used these to age 22 African elephant foetuses collected during culling operations. Pregnancy can be first recognized ultrasonographically by day 50, the presumptive yolk sac by about day 75 and the zonary placenta by about day 85. The trunk is first recognizable by days 85–90 and is distinct by day 104, while the first heartbeats are evident from around day 80. By combining ultrasonography and morphology, we have been able to produce the first reliable criteria for estimating gestational age and ontological development of Asian and African elephant foetuses during the first third of gestation.

Keywords: ultrasonography; foetal growth; foetal development; Proboscidea; gestation

1. INTRODUCTION

There are three recognized elephant species: the African savannah elephant (*Loxodonta africana*); the African forest elephant (*Loxodonta cyclotis*); and the Asian elephant (*Elephas maximus*; Roca *et al.* 2001). Their gestation length is the by far longest of all mammals (623–729 days in the Asian and 640–673 days in the African elephant; Sukumar 2003; Meyer *et al.* 2004). The Asian elephant is regarded as an endangered species in the wild (Sukumar 2003), and captive breeding may be its only hope of long-term survival. The lack of success with captive breeding of either species has made it extremely difficult to study foetal growth and development, hence research has been dependent on African elephant foetuses of unknown gestational age collected during culling operations which took place from 1967 to 1995.

Gaeth *et al.* (1999) serially sectioned one elephant embryo and six foetuses obtained from culling operations in the Kruger National Park, South Africa, between 1993 and 1995. Craig's (1984) formula was used to estimate the age of the specimens. According to this, the embryo was at 58 days of gestation and the foetuses ranged from 97 to 166 days. This is the first account of elephant organogenesis, and it revealed the unique nature of the mesonephric kidney with its nephrostomes and the reasons why the testes do not descend into a scrotum. Based on these and earlier findings, Gaeth *et al.* suggested that elephants probably have an aquatic ancestry. This is further supported by a subsequent study of foetal lung development, pleural fusion and the evolution of the trunk, which enables the elephant to snorkel (West 2001, West *et al.* 2003). The earliest descriptions of placentation in the African elephant highlighted its zonary placenta (Amoroso & Perry 1964; Perry 1974; Allen *et al.* 2003), and in an important series of papers, Allen and colleagues have defined the unusual aspects of its placental physiology and endocrinology (reviewed in Allen 2006). However, in all of these studies, foetal age could only be given as an estimate.

The only methods presently available for estimating foetal age of the elephant are the formulae of Huggett & Widdas (1951) and Craig (1984) based on a theoretical linear relationship between the cube root of foetal mass and the foetal age. The formula was $t=\omega^{1/3}/a+t_0$, where t is the foetal age in days; ω is the foetal mass in kg; a is the specific growth velocity; and t_0 is the minimal age to be determined from the equation. Huggett & Widdas arbitrarily assumed t_0 to be one-tenth of the gestation length. Perry (1953) determined that the 'specific foetal growth velocity' for both African and Asian elephants was 0.08, given that the average weight at birth is 120 kg and the gestation length is 22 months. Therefore, the

* Author for correspondence (hildebrandt@izw-berlin.de).

Received 14 August 2006
Accepted 12 September 2006

elephant equation according to Huggett & Widdas was $t=120.5\omega^{1/3}+66$. Craig (1984) modified this equation to give greater values for a and t_0 in view of his observations on foetuses collected during culling operations in Zimbabwe from 1980 to 1982. Craig concluded that the assumed specific growth velocity was too low, and he revised the formula to $t=105\omega^{1/3}+138$, assuming that prior to day 138 the foetus had a different but unknown growth velocity. Therefore, he suggested that the Hugget & Widdas equation be modified to $t=105\omega^{1/3}-(\omega^{1/3}+0.199)^{-3}+140$, to account for a much slower nonlinear growth during early gestation, despite not having any actual data on foetuses younger than 138 days of gestation.

The introduction of transrectal ultrasonography coupled with successful captive breeding programmes has opened up a whole new way of studying the reproductive biology of elephants (Hildebrandt *et al.* 1998). We have been able to produce accurate growth curves for Asian and African elephant foetuses, and follow their development from implantation until 240 days of gestation.

2. MATERIAL AND METHODS

(a) *Fixed elephant specimens*

Six formalin-fixed foetuses from the Kruger National Park Museum (water bath, WB1–6) measured in 1997, 15 African elephant foetuses (elephant foetus, EF1–15) collected during culling operations in the Kruger National Park in 1974, 1993 and 1995 and an additional foetus (EF16) collected in 1967 from a cull in the Luangwa Valley, Zambia were used in the study. The specimens were all photographed, weighed and relevant morphological measurements such as crown–rump length (CRL, distance from the vertex of the skull to the base of the tail) were taken. Specimens WB1–6 were then sonographically assessed in a water bath (3.5–10 MHz, Hitachi EUB 495) and the ultrasound scans were recorded on S-VHS tape and analysed.

(b) *Pregnant elephants*

In the period from 1995 to 2005, 9 captive African elephants (La) and 10 captive Asian elephants (Em) were examined (scanned elephants, SE1–19; table 1). In the course of artificial insemination (AI) programmes, the hormone profiles together with frequent ultrasound examinations allowed for the exact timing of ovulation. Rupturing of the leading Graafian follicle was expected 12 h after the second luteinizing hormone (LH) peak. Growth of the Graafian follicle as well as its disappearance were detected sonographically. AI was performed in most cases two to three times when the Graafian follicle was still visible and after it had disappeared. Therefore, the date of ovulation was defined by the absence of a previously enlarged Graafian follicle at the time of AI ($n=7$) or by the detection of a second LH peak measured in daily blood serum samples (Kapustin *et al.* 1996; Brown *et al.* 2004) at the time of mating. Multiple AIs were performed owing to poor semen quality. (For most of the performed AIs, the semen was collected at a different institution from where the recipient elephant cow was housed. This made long transport necessary, which had a negative impact on the semen quality.)

Table 1. Pregnant elephants monitored by transrectal ultrasound.

ID	total no. of examinations	species	date of conception	gestational age (*d*)	
SE[a]1	1	Em[b]	13 Jan 2004	NB[c]	69
SE2	1	Em	18 Jul 1994	NB	189
SE3	1	Em	19 Aug 2003	NB	216
SE4	1	Em	19 Mar 2004	AI[d]	133
SE5	1	La[e]	30 Jan 2004	NB	122
SE6	1	La	13 Aug 2001	AI	129
SE7	1	La	23 May 2001	AI	150
SE8	1	La	16 Jun 2001	AI	68
SE9	1	La	23 Aug 2001	AI	132
SE10	2	La	3 Dec 2000	AI	88–172
SE11	2	Em	22 Feb 2000	AI	97–158
SE12	3	Em	15 Apr 2995	NB	79–189
SE13	3	Em	18 Jan 1998	NB	76–130
SE14	3	La	16 Apr 2000	NB	69–110
SE15	3	Em	18 Dec 2002	NB	64–163
SE5	4	La	23 May 1999	AI	58–126
SE16	6	La	23 Jul 1999	AI	60–240
SE17	14	Em	4 Apr 2004	NB	80–234
SE18	35	Em	10 Jul 2004	NB	85–226
SE19	56	Em	27 Oct 2004	NB	47–201

[a] SE, scanned elephant. [b] Em, *Elephas maximus*. [c] NB, natural breeding. [d] AI, artificial insemination. [e] La, *Loxodonta africana*.

(c) *Ultrasonography*

During the first third of pregnancy, sonographic examinations were performed transrectally using the technique of Hildebrandt *et al.* (2000). Some elephants were in the standing position and others in lateral recumbency, as previously described (Hildebrandt *et al.* 2000).

Later in gestation, transcutaneous ultrasound was applied (Hildebrandt *et al.* 2006). In most cases, portable B-mode real-time ultrasound systems (Sonosite, Inc. USA; EUB 459, Hitachi Medical Corporation, Japan) with a transducer frequency range from 10.0 to 2.0 MHz were employed. Three elephants were assessed with stationary three-dimensional ultrasound systems (Voluson 530 and Voluson 730, GE Medical Systems, Austria) equipped with 7.0–4.0 MHz transducers. All ultrasound examinations were videotaped on analogue S-VHS or digital tapes for retrospective analysis. Three-dimensional scans were stored on magneto-optical discs.

(d) *Retrospective analysis of the ultrasound data and measurements*

All ultrasound recordings (WB1–6 and SE1–19) were analysed retrospectively. For the measurement of different biometric parameters, such as CRL, biparietal diameter (BPD), thoracic diameter (THD) and femur length (FL), three-dimensional sonograms had to be created from the two-dimensional recordings (Adobe Premiere Pro 1.5, Adobe Systems Inc., USA) before foetal structures could be measured with a special software program (AnalySIS v. 3.1, Olympus, Germany).

By working with the three-dimensional technique, biometric measurements could be derived directly from the scans (4D View, GE Medical Systems, Austria). In the earliest embryos, where there was no bone ossification, the length of the embryo on its longest axis was defined as the CRL. In the later stages, the CRL was measured as the distance from the

Table 2. Data collected from fixed African elephant (*Loxodonta Africana*) specimens.

ID	indirect, sonographic CRL measurement (mm)	direct CRL measurement (mm)	head length (mm)	mass (g)	calculated age from formula (3.4) (days)	calculated age from formula (3.7) (days)
EF[a]1		5.4	1.5	0.04	60	60
EF2		18.5	8.8	0.8	82	81
EF3		19.0	9.9	1.3	82	85
EF4		17.6	9.7	1.5	81	86
EF5		27.5	12.7	2.6	92	92
EF6		36.4	17.5	4.0	100	97
EF7		39.5	15.7	6.6	103	103
WB[b]1	30.2	33.0	11.4	7.2	97	103
EF8		46.4	22.8	9.2	109	107
EF9		61.4	24.9	17.0	120	115
EF10		59.5	25.0	18.5	119	117
WB2	64.5	66.8	20.8	24.4	123	121
WB3	73.3	78.1	30.6	47.8	131	132
EF11		112.4	48.7	107.0	150	147
EF12		113.4	49.0	113.7	150	148
EF13		116.1	50.6	114.6	152	148
WB4	120.0	116.0	43.1	133.7	152	151
EF14		123.2	52.3	168.6	155	156
EF15		124.9	55.0	205.1	156	160
WB5	140.0	146.2	50.3	288.1	166	168
EF16		150.0	65.8	299.8	167	169
WB6	180.0	185.5	59.0	554.3	182	184

[a] EF, elephant foetus.
[b] WB, water bath.

vertex of the skull to the base of the tail, as in the fixed specimens. The CRL was preferably measured from a lateral scan of the foetus. If that could not be achieved, the CRL was obtained from a horizontal section. Sometimes it was not possible to image the complete CRL of the foetus in one frame, so the lengths of the head and the torso were combined.

The BPD of the foetal head was measured from the outer margin of one parietal bone to the other. The FL was defined as the maximal length of the diaphysis. The THD was the maximal diameter of the rib cage in the horizontal section.

(e) *Statistics*

Curvilinear regression analyses were used to establish relationships between the age of the foetuses and their morphological parameters. Analysis of covariance was used to compare the regression lines for Asian and African elephants. The curve fits were performed with TableCurve 2D v. 5 (AISN Software, Inc. Mapleton, OR, USA). All other statistical calculations were performed using the SPSS v. 12.0 (SPSS Inc., Chicago, IL, USA) statistical software package.

3. RESULTS

(a) *Validation of ultrasound measurements*

Data collected from foetal elephant specimens (WB1–6 and EF1–16) of different developmental stages are listed in table 2. In order to test the reliability of the ultrasound measurements, the CRLs of six foetuses (WB1–6) were measured directly and indirectly by ultrasound in a water bath. The results of the two methods did not differ significantly (regression through the origin: $\mathrm{CRL} = 1.026 \times \mathrm{CRL}_{\mathrm{ultrasound}}$, $R^2 = 0.999$, $p < 0.001$; 95% CI of slope: 0.999–1.1060).

(b) *New mathematical models for foetal growth using ultrasound data*

Since the dates of ovulation of SE1–19 were known, each ultrasound measurement could be assigned a known gestational age. The CRL was an accessible parameter from 62 to 202 days of gestation and ranged from 5.0 to 205.3 mm. It became more difficult to measure with increasing growth of the foetus and its varying flexure. BPD could be measured transrectally from 83 to 226 days of gestation, and it ranged from 7.7 to 91.3 mm. THD ranged from 10.5 to 88.0 mm between days 99 and 240. FL was a parameter that could only be determined later in gestation. It ranged from 6.4 to 58.0 mm and could be reliably measured from 119 to 234 days of gestation. Regression models were fitted to the data in order to construct mean curves for age and CRL, BPD, THD and FL (figure 1*a*). The data were examined to see if the foetal growth rates differed between Asian and African elephants. No significant differences in the slopes or the intercepts were observed between Asian and African elephants (age with $\mathrm{CRL}^{1/2}$: $p(\text{slopes}) = 0.091$, $p(\text{intercepts}) = 0.947$; age with BPD: $p(\text{slopes}) = 0.405$, $p(\text{intercepts}) = 0.751$; age with THD: $p(\text{slopes}) = 0.522$, $p(\text{intercepts}) = 0.647$; age with FL: $p(\text{slopes}) = 0.890$, $p(\text{intercepts}) = 0.979$). Therefore, all subsequent calculations were performed using the combined data for both species. The regression analyses yielded the following equations:

$$\text{age} = 78.98 + 1.95 \times \text{BPD},\ R^2 = 0.95,\ F(1, 105) = 2195.5,\ p < 0.001, \tag{3.1}$$

$$\text{age} = 85.32 + 1.69 \times \text{THD},\ R^2 = 0.98,\ F(1, 76) = 3640.7,\ p < 0.001, \tag{3.2}$$

$$\text{age} = 113.55 + 2.02 \times \text{FL},\ R^2 = 0.97,\ F(1, 54) = 1467.2,\ p < 0.001. \tag{3.3}$$

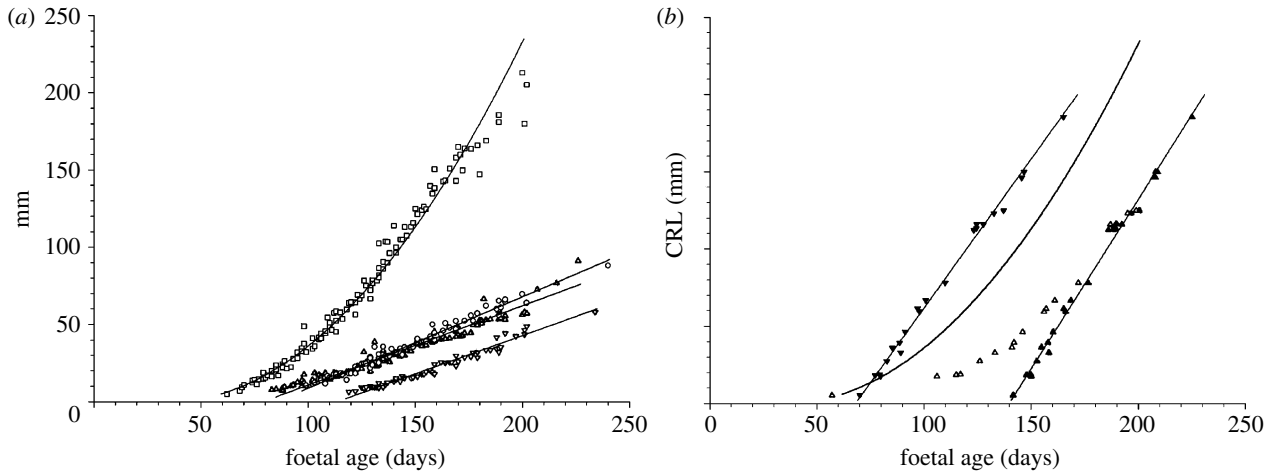

Figure 1. (*a*) Foetal growth curves based on ultrasound measurements. The ultrasound data (SE1–19) show the relationship between true gestation age and crown–rump length (CRL). Crown–rump length (open square), biparietal diameter (open up triangle), thoracic diameter (open circle) and femur length (open down triangle) are plotted against foetal age. (*b*) Evaluation of existing models for the determination of foetal age. The foetal specimens (WB1–6 and EF1–16) have been aged using our formula (3.4) (solid line), the formulae by Huggett/Widdas (filled down triangle) and Craig for under 138 days (open up triangle) and Craig for over 140 days (filled up triangle), respectively.

The relationship between CRL and age is nonlinear, and it can be adequately fitted by a square root function

$$\text{age} = 35.14 + 10.80 \times \text{CRL}^{1/2},\ R^2 = 0.98,\ F(1,114) = 5936.67,\ p < 0.001. \tag{3.4}$$

The 95% prediction band around the regression curve (3.4) (not shown) is expected to enclose 95% of future data points, thus indicating the precision of future estimations. The prediction band boundaries are in a vertical distance between ± 9.2 and ± 9.7 days (standard deviation (s.d.)) from the regression curve for CRL ≥ 5 mm or ≤ 213 mm.

Existing formulae for foetal age determination describe the relationship between foetal mass and foetal age. Since foetal mass cannot be determined for living foetuses, we used the CRL–age data assessed by ultrasound for comparative purposes. For this, data from foetal elephant specimens (WB1–6 and EF1–16) comprising both foetal CRL and foetal mass measurements were used. Foetal age for these specimens was calculated on the basis of foetal mass according to Huggett/Widdas (using the foetal growth velocity as determined by Perry 1953) and Craig. We then supplemented the CRL–age plot of these estimations by the regression line of formula (3.4), which is derived from our ultrasound data (figure 1*b*). The Huggett/Widdas formula (using the foetal growth velocity as determined by Perry 1953) gave ages that were approximately 20 days younger than the known age (figure 1*b*). In contrast, both Craig formulae overestimated foetal age by 25–65 days, with the exception of the age calculated for the youngest embryo using the formula developed for younger foetuses (figure 1*b*). Therefore, we derived a new formula to describe the age–mass relationship, based on our ultrasound measurements. Using the data from all the foetal elephant specimens (WB1-6 and EF1-16), a linear regression of the cube root of foetal mass ω (g) against foetal CRL (mm) revealed

$$\text{CRL} = 23.10 \times \omega^{1/3} - 3.28,\ R^2 = 0.99,\ F(1,20) = 3177.7,\ p < 0.001. \tag{3.5}$$

To substitute the CRL in equation (3.4) by that of equation (3.5) would result in a complicated mass–age formula with four different parameters. Therefore, we estimated the age of the foetal elephant specimens from the CRL measurements (WB1–6 and EF1–16) using equation (3.4) in order to find a simpler age–mass relationship (figure 1*b*). The formulae used by Huggett/Widdas and Craig assume a linear relationship between the cube root of foetal mass ω and the foetal age. However, the relationship is nonlinear. A square root function provides an adequate fit, resulting in the equations

$$\text{age} = 28.434 + 54.20 \times ((\text{mass})^{1/3})^{1/2},\ R^2 = 0.99,\ F(1,20) = 3177.7,\ p < 0.001, \tag{3.6}$$

or

$$\text{age} = 28.434 + 54.20 \times (\text{mass})^{1/6}. \tag{3.7}$$

Thus, our formulae are accurate up to at least 202 ± 9.7 days (s.d.).

(c) *Foetal growth from observations of fixed foetal elephant specimens*

As would be expected, the CRL, head, tail and trunk lengths increased with increasing body mass. In some cases where foetuses were of similar mass, the heavier foetus sometimes had shorter crown–rump, head, tail and trunk lengths. For example, foetuses EF3 and 4 were of similar mass—1.32 and 1.46 g, respectively—yet EF3 was longer in CRL (19 mm compared to 17.6 mm), head length (9.9 mm compared to 9.7 mm) and in tail length (2 mm compared to 1.3 mm). The average length of the hind limbs was always shorter than the average length of the forelimbs, as is observed in adult elephants. Head length was 28% of the CRL of EF1. This increased with age to 55% of EF4 and then decreased with age to plateau at around 42–44%.

(d) *Developmental milestones related to foetal age*

Sonographic imaging of foetuses of known age, coupled with the description of the gross morphology of foetal specimens with the calculated age according to equation (3.4), have allowed the definition of ontogenetic milestones for the elephant during the first 167 days of gestation (table 3). On day 46, there was evidence of constrained, oval-shaped fluid accumulation within the

Table 3. Developmental milestones in the African elephant.

days of gestation	milestone
50	blastocyst sonographically visible
60	head-fold stage
74	presumptive yolk sac sonographically visible
80	first heartbeat detectable
80–85	zonary placenta sonographically visible
86–95	macroscopic signs of trunk development
95	distinct dilatation of physiological midgut herniation
92–100	body lengthens and straightens
105	trunk distinct
120	herniation disappears
118–120	tip of the trunk with finger-like projections
167	large ears extending over neck

uterine lumen detected by ultrasound. However, the typical white 'enhancement' lines were not observed. Only on day 50 of gestation could a clear embryonic vesicle be located and identified by ultrasound scanning. By that time, a spherical fluid-filled embryonic vesicle was visible within the lumen of the uterine horn, close to the uterine body (figure 2*a*). The embryo itself was initially detected as a small dot in close proximity to the uterine wall on day 62 of gestation. It changed into a more oblong structure by day 74 (figure 2*b*) and was attached to a distinct echogenic round foetal membrane, the presumed yolk sac. The development of the amnion and the allantoic membrane were difficult to visualize. A second more delicate, less echogenic membrane was detected around days 85–95, enclosing both the embryo and the yolk sac. The second membrane is presumed to be the allantois.

The youngest fixed specimen (EF1), calculated to be at 60 days of gestation, was a head-fold stage embryo (figure 3*a*). Approximately 35 somites extended from the base of the head to the end of the tail. The two branchial arches and the optic placodes were easily distinguishable on the head. The forelimb buds and the much smaller hind-limb buds protruded from each side of the embryo. The blood in the atria of the developing heart was clearly visible.

On ultrasound, the pulsating heart was the most prominent organ observed in the early embryo. The embryonic heartbeat could first be detected on day 80 of gestation, shortly followed by the differentiation of the head and the rump between 83 and 85 days of gestation. The first signs of trunk development were seen around days 90–98, when the nose was triangular, defined by two hyperechoic white lines (figure 2*c*). A beak-like trunk was also observed in elephant specimens EF2–4 (calculated 81–82 days of gestation; figure 3*b*). All three of these specimens had a cervical flexure of about 90° at the level of the hindbrain, and the hind-, mid- and forebrains were easily distinguishable. The neural tube was not yet completely fused anteriorly. Pigment was visible surrounding the developing lens. The ears were small and caudally placed in the neck region. The fore- and hind limbs were flexed at the carpals and the tarsals, respectively.

The development of the placenta was first visible ultrasonographically by an endometrial reaction indicated by the tissue layers of higher echodensity on day 80. In cross-section, placental tissue protruded in the chorioallantoic cavity beginning on day 85 of gestation. Paired allantoic vessels, consisting of a vein and an artery, supplied the placenta. The characteristic blood vessels could be seen with colour Doppler flow. From day 126 of gestation onwards, mushroom-like structures, the so-called allantoic pustules, could be depicted by ultrasound on the foetal side of the allantoic membranes (figure 2*h*).

A distinct dilatation of the umbilical cord could be seen from day 95 of gestation (figure 2*d*). This transient phenomenon is well known in human obstetrics and is referred to as physiological midgut herniation, marking a period where the rapidly growing liver occupies most of the abdomen, so that parts of the elongated midgut protrude into the umbilical cord. With increasing growth and lengthening of the foetus, the midgut retreats back into the abdomen and the herniation vanishes. By ultrasound, the physiological midgut herniation could be observed until day 120 of gestation, and it was also observed in EF7 (103 days of calculated gestation), where a bulge of intestinal loops could be identified within the umbilical cord (figure 3*f*).

By 92–100 days of gestation, the bodies had straightened and lengthened, and the degree of flexure of the heads was reduced in the fixed foetuses EF5 and 6 (figure 3*c*,*d*). The heads comprised almost half of the total body length. The superficial vascular plexus was visible on the scalp of EF5 (figure 3*c*). The toes were distinguishable on all of the limbs. The base of the tails was more defined than in the younger foetuses. Anteriorly, the neural tube had not yet closed (figure 3*e*).

In EF7 (103 days of gestation), wrist and elbow joints in the forelimbs, and ankle and knee joints in the hind limbs, had formed. The erect head merged into a distinct neck and now comprised less than 50% of the foetal body length. Eyelids had formed over the eyes. Fusion of the neural tube was not yet completed anteriorly. The gut was herniated at the umbilicus.

From day 106 of gestation, clear sonoluscent brain structures with the surrounding ventricles could be depicted by ultrasound (figure 2*e*). With increasing growth, other internal structures, such as the borderline between lung and liver, the kidneys and the gastric vesicle, could also be visualized. Foetal blood circulation was depicted by colour Doppler flow (figure 2*f*).

At 119–120 days of gestation (EF9 and 10), the head now comprised approximately 40% of the total body length. The tip of the trunk of EF9 had two finger-like projections, ventral and dorsal, characteristic of the adult African elephant, but these were not observed in the trunk of EF10. The neural tube had fused completely.

Between 150 and 156 days of gestation (EF11–15; figure 3*g*), all foetuses were very similar in appearance with only 1.25 cm separating them in CRL. This stage of development is characterized by a rapid growth and weight gain. The legs of the foetuses appeared much longer than in the earlier foetuses. There were two finger-like projections, ventral and dorsal, at the tips of all the trunks. The muscles of the hindquarters outlined the rump. The foetuses were lean, with the exception of EF15. EF15 weighed much more than foetuses EF11–14, but only differed slightly in CRL.

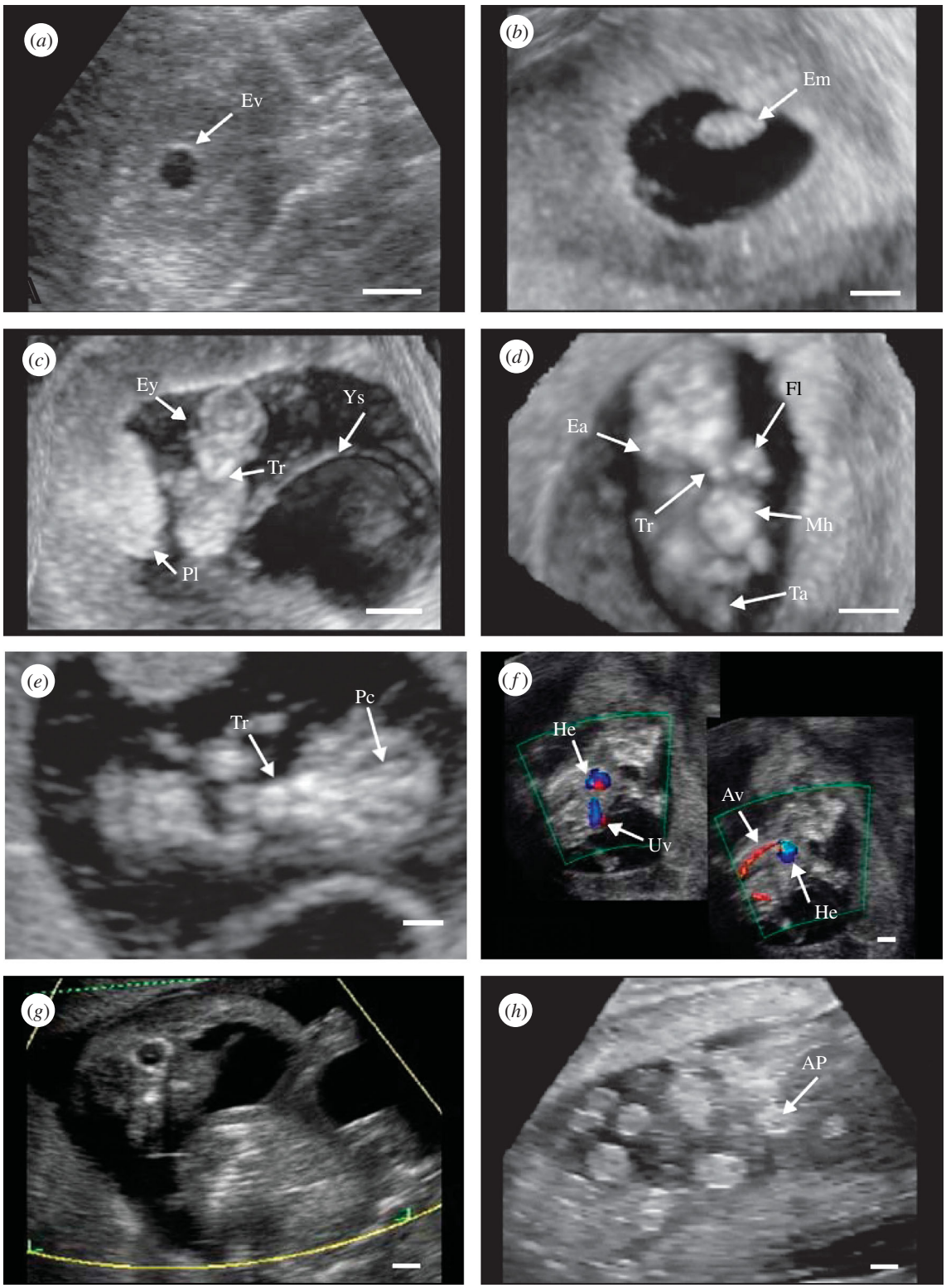

Figure 2. Sonographic milestones. (*a*) Embryonic vesicle (Ev) at day 50. (*b*) An early embryo at day 74 of gestation. (*c*) Three-dimensional reconstruction of an embryo at 97 days of gestation with its yolk sac (Ys). The eyes (Ey) and the beak-like trunk (Tr) are clearly depicted. The placenta (Pl) is well developed. (*d*) Three-dimensional reconstruction of an early foetus of 102 days of gestation showing the physiological midgut herniation (Mh). The right ear (Ea), the typical trunk (Tr) and one fore limb (Fl) are easy to recognize. (*e*) At 108 days of gestation, the echogenic plexus choroideus (Pc) already fills most of the lateral ventricle. The trunk (Tr) is positioned between the fore limbs. (*f*) Characterization of foetal circulation at day 126 of gestation. The foetal heart (He), arteria vertebralis (Av) and umbilical vessels (Uv) are outlined by colour Doppler flow. (*g*) Lateral position of the foetus at 133 days of gestation. (*h*) In the later stages of pregnancy, here at day 303 of gestation, the allantoic pustules (AP) protrude into the allantoic cavity. Scale bars, 1 cm.

The second largest of the fixed foetuses, EF16 (calculated 167 days of gestation), had large ears extending back over the neck (figure 3*h*). On both sides of the head, rounded masses of tissue beneath the skin were easily identified between the eye and the ear. These were thought to be the temporal glands. The trunk had furrows at its base and the tip of the trunk had dorsal and ventral finger-like processes. The chin was still identifiable

Figure 3. African savannah elephant embryo and foetuses. (*a*) EF1 (60 days of gestation). a, amnion; ba, branchial arches; fl, fore limb; h, heart; oe, optic evagination; s, somites; ta, tail; t, trunk. Scale bar, 0.25 cm. (*b*) EF4 (81 days of gestation). (*c*) EF5 (92 days of gestation). (*d*) EF6 (97 days of gestation). (*e*) Dorsal aspect of EF6 (100 days of gestation) showing the extent of neural tube development. (*f*) EF7 (103 days of gestation). (*g*) EF11 (150 days of gestation). (*h*) EF16 (167 days of gestation). Scale bars, 1 cm. Panel (*a*) from Gaeth *et al.* (1999).

from the lower lip, a feature not seen in adult elephants. The small invaginations of the mammary primordia were between the front legs. The soles of the feet were rounded, and there were three nails and one forming on each of the forefeet and three nails on each of the hind feet. There were no body or tail hairs.

After 240 days of gestation, foetuses could no longer be visualized by transrectal ultrasound. However, transcutaneous ultrasound was possible in the middle of the second third of pregnancy. Foetal hair, heartbeat, rib cage and skull could be seen, as well as the free allantoic membranes and the allantoic pustules (figure 2*h*).

4. DISCUSSION

The present study describes the first longitudinal monitoring of known-age Asian and African elephant foetuses by ultrasound. This is also the first accurate description of the ontogenetic development of a series of elephant foetuses in the first third of pregnancy. Foetal growth was monitored by relating ultrasound measurements such as CRL, BPD, THD and FL to a known foetal age. The fact that these biometric parameters were always closely correlated with foetal age confirms the accuracy of the timing of conception. The date of ovulation was determined by the disappearance of the previously observed Graafian follicle in AI programmes or by the detection of a second LH surge in daily blood samples associated with mating. Owing to individual variability in gestation lengths (± 46 days in the Asian and ± 16 days in the African elephant; Meyer *et al.* 2004), the time of ovulation cannot be accurately inferred from the date of birth. Observations of mating in captivity without reference to hormonal profiles are also an unreliable method of timing gestation (Eisenberg *et al.* 1971). All our observations are critically dependent on knowing the precise timing of the day of ovulation.

New formulae for foetal age determination have been developed based on ultrasound measurements of CRL, BPD, THD and FL. Developmental milestones as seen by ultrasound were correlated with development directly observed in fixed specimens. Pregnancy could be confirmed by ultrasound after about 50 days of gestation, when the blastocyst began to distend the uterine lumen. The embryo itself was not detected until day 62 of gestation. Between days 74 and 85, foetal membranes, presumed to be the yolk sac and the allantois, respectively, became sonographically visible. One embryo in Amoroso & Perry's (1964) study had a discernable yolk sac, similar to those seen in our ultrasound images. Using our formulae, we can now say that the 2 g (4 cm CRL) embryo of Amoroso & Perry was approximately 103 days old, not one to two months they estimated, but the yolk sac was already regressing. Amoroso & Perry (1964) report that in their 10 g (10 cm CRL) foetus, the yolk sac was no longer visible and the extra-embryonic coelom was obliterated by the fusion of the allantois with the chorion. Comparing this 10 cm CRL foetus with the specimens of our study, we believe that there was a typographical error and that the 10 cm CRL foetus actually weighed 100 g. According to our formula (3.4), which is based on the CRL, the age of a 10 cm CRL foetus would be 143 days and according to our formula (3.7), which is based on mass, the 10 g foetus would be 108 days old and a 100 g foetus would be 145 days old. Furthermore, with ultrasound, the yolk sac is still visible at 108 days, but they report that the yolk sac had disappeared, thus their 10 g foetus must actually weigh 100 g.

With advancing gestation, the head and rump of the embryo became more pronounced (83 days of gestation), shortly followed by the development of fore- and hind limbs, ears and the characteristic elephant trunk (days 86–90 of gestation), whose early appearance suggests that it is a phylogenetically ancient trait of the elephant. Between days 95 and 120, a dilatation of the umbilical cord close to the abdominal wall was observed by ultrasound. This physiological midgut herniation is similar to that seen in developing human foetuses (Warren *et al.* 1989). It was also detected in two of the fixed elephant specimens (EF7, 103 days of gestation, and WB2, 121 days of gestation). On days 82–100 of gestation, a lengthening of the body and the fragmentation of the brain in fore-, mid- and hindbrains were apparent in EF2–6. In EF7, the eyelids had formed and by 119–120 days (EF9 and 10), the body flexure had further reduced. The neural tube had fused completely. If the key criteria from human embryology are used, it appears that embryogenesis in the elephant is completed by 100–120 days of gestation. Subsequent development was characterized by rapid foetal growth and further differentiation of the organs. Not surprisingly, fine morphological details were noted earlier in the fixed specimens of equivalent ages than in the foetuses assessed by ultrasound.

There was a significant difference between our direct measurements of foetal age and the previous mathematical estimates. The Huggett & Widdas (1951) formula underestimated foetal age, whereas both of Craig's (1984) formulae overestimated foetal age. Although the slope of all three graphs is very similar, the starting point differs. The Huggett/Widdas and Craig formulae are dependent on a hypothetical intercept with the time axis, which does not reflect actual foetal growth. With our newly developed formulae (3.1)–(3.7), gestational age can be accurately determined for at least 202 ± 9.7 days. We do not know the rate at which foetal growth takes place later in gestation. However, it is known from other mammalian species that growth curves based on the CRL are S-shaped (Evans & Sack 1973). Therefore, we assume that CRL increases at a much slower rate, while foetal mass increases more rapidly in the last third of pregnancy.

From the observations in EF3 and 4, we know that foetuses with similar masses can differ in relation to crown–rump, head, tail and trunk lengths, although some of these differences may be due to fixation artefacts. Mass is not an ideal parameter for determining foetal age, as mass cannot be determined in living foetuses. Therefore, the ultrasound approach of measuring CRL makes elephant foetal aging possible. Thus, the new formulae (3.1)–(3.7) combined with ultrasonography provide the first reliable criteria for recording gestational age and ontogeny of the elephant foetus.

We thank Ian Whyte, Kruger National Park, for his assistance with the collection of the elephant foetuses from culled animals. We also thank the staff at the different elephant keeping institutions for their great support. The DAAD (Deutscher Akademischer Austauschdienst) provided financial support for the ultrasound assessments of three pregnant elephants at the African Lion Safari, Canada.

REFERENCES

Allen, W. R. 2006 Ovulation, pregnancy, placentation and husbandry in the African elephant (*Loxodonta africana*). *Phil. Trans. R. Soc. B* **361**, 821–834. (doi:10.1098/rstb.2006.1831)

Allen, W. R., Mathias, S., Wooding, F. B. & van Aarde, R. J. 2003 Placentation in the African elephant (*Loxodonta africana*): II Morphological changes in the uterus and placenta throughout gestation. *Placenta* **24**, 598–617. (doi:10.1016/S0143-4004(03)00102-4)

Amoroso, E. C. & Perry, J. S. 1964 The foetal membranes and placenta of the African elephant (*Loxodonta africana*). *Phil. Trans. R. Soc. B* **248**, 1–34.

Brown, J. L., Walker, S. & Moeller, T. 2004 Comparative endocrinology of cycling and non-cycling Asian (*Elephas maximus*) and African (*Loxodonta africana*) elephants. *Gen. Comp. Endocrinol.* **136**, 360–370. (doi:10.1016/j.ygcen.2004.01.013)

Craig, G. C. 1984 Foetal mass and date of conception in African elephants: a revised formula. *S. Afr. J. Sci.* **80**, 512–516.

Eisenberg, J. F., McKay, G. M. & Jainudeen, M. R. 1971 Reproductive behaviour of the Asiatic elephant (*Elephas maximus maximus* L.). *Behaviour* **38**, 193–225.

Evans, H. E. & Sack, W. O. 1973 Prenatal development of domestic and laboratory mammals: growth curves, external features and selected references. *Anat. Histol. Embryol.* **2**, 11–45.

Gaeth, A. P., Short, R. & Renfree, M. B. 1999 The developing renal, reproductive, and respiratory system of the African elephant suggest an aquatic ancestry. *Proc. Natl Acad. Sci. USA* **96**, 5555–5558. (doi:10.1073/pnas.96.10.5555)

Hildebrandt, T. B., Goeritz, F., Stetter, M. D., Hermes, R. & Hofman, R. R. 1998 Application of sonography in vertebrates. *Zoology* **101**, 200–209.

Hildebrandt, T. B., Goeritz, F., Pratt, N. C., Brown, J. L., Montali, R. J., Schmitt, D. L., Fritsch, G. & Hermes, R. 2000 Ultrasonography of the urogenital tract in elephants (*Loxodonta africana* and *Elephas maximus*): an important tool for assessing female reproductive function. *Zool. Biol.* **19**, 321–332. (doi:10.1002/1098-2361(2000)19:5<321::AID-ZOO4>3.0.CO;2-K)

Hildebrandt, T. B. 2006 Reproductive and diagnostic ultrasonography. In *Biology, medicine, and surgery of elephants* (ed. M. Fowler & S. Mikota), pp. 357–376, 1st edn. Ames, IA: Blackwell Publishing.

Huggett, A. S. & Widdas, W. 1951 The relationship between mammalian foetal weight and conception age. *J. Physiol.* **114**, 306–317.

Kapustin, N., Critzer, J., Olson, D. & Malven, P. V. 1996 Nonluteal estrous cycles of 3-week duration are initiated by anovulatory luteinizing hormone peaks in African elephants. *Biol. Reprod.* **55**, 1147–1154. (doi:10.1095/biolreprod55.5.1147)

Meyer, J. M., Walker, S., Freeman, E. W., Steinetz, B. G. & Brown, J. L. 2004 Species and fetal gender effects on endocrinology of pregnancy in elephants. *Gen. Comp. Endocrinol.* **138**, 263–270. (doi:10.1016/j.ygcen.2004.06.010)

Perry, J. S. 1953 The reproduction of the African elephant, *Loxodonta africana*. *Phil. Trans. R. Soc. B* **237**, 11–149.

Perry, J. S. 1974 Implantation, foetal membranes and early placentation of the African elephant, *Loxodonta africana*. *Phil. Trans. R. Soc. B* **269**, 109–135.

Roca, A. L., Georgiadis, N., Pecon-Slattery, J. & O'Brien, S. J. 2001 Genetic evidence for two species of elephant in Africa. *Science* **293**, 1473–1477. (doi:10.1126/science.1059936)

Sukumar, R. 2003 *The living elephants: evolutionary ecology, behaviour and conservation*, p. 478. Oxford, UK: Oxford University Press.

Warren, W. B., Timor-Tritsch, I., Peisner, D. B., Raju, S. & Rosen, M. G. 1989 Dating the early pregnancy by sequential appearance of embryonic structures. *Am. J. Obstet. Gynecol.* **161**, 747–753.

West, J. B. 2001 Snorkel breathing in the elephant explains the unique anatomy of its pleura. *Respir. Physiol.* **126**, 1–8. (doi:10.1016/S0034-5687(01)00203-1)

West, J. B., Zhenxing, F., Gaeth, A. P. & Short, R. V. 2003 Fetal lung development in the elephant reflects the adaptations required for snorkelling in adult life. *Respir. Physiol. Neurobiol.* **138**, 325–333. (doi:10.1016/S1569-9048(03)00199-X)